

See discussions, stats, and author profiles for this publication at: <https://www.researchgate.net/publication/231661767>

# Gas-Phase Chemistry of the Sulfur Hexafluoride Fragment Ions $\text{SF}_n^+$ ( $n = 0-5$ ) and $\text{SF}_n^{2+}$ ( $n = 2, 4$ ). Ab Initio Thermochemistry of Novel Reactions of $\text{S}^{+\bullet}$ and $\text{SF}^+$

ARTICLE in THE JOURNAL OF PHYSICAL CHEMISTRY A · JUNE 1998

Impact Factor: 2.69 · DOI: 10.1021/jp980876g

---

CITATIONS

15

---

READS

11

4 AUTHORS, INCLUDING:



Maria Anita Mendes

University of São Paulo

69 PUBLICATIONS 1,308 CITATIONS

SEE PROFILE

# Gas-Phase Chemistry of the Sulfur Hexafluoride Fragment Ions $\text{SF}_n^+$ ( $n = 0-5$ ) and $\text{SF}_n^{2+}$ ( $n = 2, 4$ ). Ab Initio Thermochemistry of Novel Reactions of $\text{S}^{+\bullet}$ and $\text{SF}^+$

Regina Sparrapan, Maria Anita Mendes, Isabel P. P. Ferreira, and Marcos N. Eberlin\*

Institute of Chemistry, State University of Campinas-UNICAMP, CP 6154, 13083-970 Campinas, SP, Brazil

Cristiano Santos and José Carlos Nogueira†

Department of Chemistry, Federal University of São Carlos-UFSCar, São Carlos, SP, Brazil

Received: January 23, 1998; In Final Form: April 23, 1998

A systematic study of the gas-phase chemistry of the major positively charged ions produced by 70 eV dissociative electron ionization of  $\text{SF}_6$ , i.e.,  $\text{SF}_n^+$  ( $n = 0-5$ ) and  $\text{SF}_n^{2+}$  ( $n = 2, 4$ ), has been performed via pentaquadrupole (QqQqQ) mass spectrometric experiments in conjunction with G2(MP2) ab initio calculations. Comparison, under exactly the same 15 eV collision conditions, of the  $\text{SF}_n^+$  proclivities to dissociate by F loss was accomplished via a *tandem-in-space* three-dimensional MS<sup>2</sup> scan. The experimental  $\text{SF}_n^+$  dissociation proclivities were found to correlate perfectly with those expected from G2(MP2) dissociation thresholds. Ion/molecule reactions of mass-selected  $\text{SF}_n^+$  and  $\text{SF}_n^{2+}$  were performed with  $\text{O}_2$  and the oxygenated neutral gases  $\text{H}_2\text{O}$ ,  $\text{CO}$ ,  $\text{CO}_2$ , and  $\text{N}_2\text{O}$ . The ions, under the very low energy (near zero) multiple collision conditions employed, undergo either dissociation by F loss or charge exchange, or participate in novel reactions that have been corroborated by both MS<sup>3</sup> experiments and G2(MP2) ab initio thermochemistry. O-abstraction takes place in reactions of  $\text{SF}^+$  with  $\text{O}_2$  and  $\text{CO}$ , and of  $\text{S}^{+\bullet}$  with  $\text{CO}_2$  and  $\text{O}_2$ , and the corresponding oxyions  $\text{F-SO}^+$  and  $\text{SO}^{+\bullet}$  are formed to great extents. CO-abstraction that yields ionized carbon oxysulfide ( $\text{COS}^{+\bullet}$ ) also occurs to a minor extent in reactions of  $\text{S}^{+\bullet}$  with  $\text{CO}_2$ . Reactions of  $\text{SF}^+$  with  $\text{CO}$  yields a minor  $\text{COS}^{+\bullet}$  product in a net sulfur cation ( $\text{S}^{+\bullet}$ ) transfer reaction. Theory corroborates the experimental observations as the respective O-abstraction and  $\text{S}^{+\bullet}$  transfer reactions are predicted by G2(MP2) ab initio thermochemistry to be the most favorable processes.

## Introduction

The study of the fundamental properties and practical applications of the fascinating hypervalent sulfur hexafluoride molecule ( $\text{SF}_6$ ) has been of great diversity and renewed interest for several decades.<sup>1-7</sup>  $\text{SF}_6$  displays high chemical stability and excellent insulating properties; hence, it has found widespread use as a highly efficient insulator in the electric power industry.<sup>1</sup>  $\text{SF}_6$  is also used as the source of F atoms in lasers, as well as in a number of plasma-etching processes in the semiconductor industry.<sup>2</sup>  $\text{SF}_6$  also has been shown to be useful as an electron capture reagent in the source of high-pressure mass spectrometers,<sup>3</sup> and it has been applied for isotope separation by laser irradiation<sup>4</sup> and multiphoton processes.<sup>5</sup> The  $\text{SF}_6$  molecule has also served as a model for  $\text{UF}_6$  used in uranium isotope enrichment<sup>6</sup> and as a model for hypervalent species<sup>7</sup> in which bonding well exceeds those predicted on the basis of the Langmuir–Lewis theory.<sup>8</sup>

Despite the great chemical stability of neutral  $\text{SF}_6$ , its ionized form is unstable with respect to  $\text{SF}_5^+$  and  $\text{F}^+$ ; hence  $\text{SF}_6^{+\bullet}$  cannot be sampled owing to its rapid dissociation.<sup>9</sup> The  $\text{SF}_6^{+\bullet}$  fragment ions  $\text{SF}_n^+$  and  $\text{SF}_n^-$  ( $n = 0-5$ ) are, however, stable gaseous species and are formed abundantly upon dissociative electron ionization (EI) of  $\text{SF}_6$ .  $\text{SF}_n^{+(-)}$  ions are also formed as byproducts when  $\text{SF}_6$  is used as a gaseous dielectric or in plasma-etching gases.<sup>10</sup> An interesting application of  $\text{SF}_n^+$  is

their implantation into GaAs field-electron transistors to improve performance.<sup>11</sup>

Owing to the great practical as well as fundamental importance of  $\text{SF}_6$ , a variety of theoretical<sup>9</sup> and experimental studies have been conducted on neutral  $\text{SF}_6$  and its ionic fragments. Gas-phase studies on the chemistry of neutral  $\text{SF}_6$ <sup>12-14</sup> and the  $\text{SF}_n^+$  and  $\text{SF}_n^-$  ( $n = 0-5$ ) ions<sup>15-23</sup> have been, however, generally sporadic and scattered, and only a few systematic studies have been carried out. Such systematic studies would be invaluable for achieving deeper insights into the intrinsic reactivities and bonding natures of  $\text{SF}_6$  and its  $\text{SF}_n^{+(-)}$  ions, and particularly to better rationalize and control the chemical and electrical processes in which sulfur hexafluoride ions are involved.

Owing in part to the protective layer of F atoms<sup>12</sup> that obstructs the access to the reactive S center, neutral  $\text{SF}_6$  is a quite chemically inert species, and gas-phase studies have shown few ion/molecule reactions in which neutral  $\text{SF}_6$  participates. Either  $\text{F}^-$  abstraction or dissociative charge exchange that affords mainly  $\text{SF}_5^+$  occurs in reactions of  $\text{SF}_6$  with a series of cations that have ionization energies higher than that of  $\text{SF}_6$ .<sup>13</sup> However, early transition metal cations such as  $\text{Sc}^+$  that have at least one empty d orbital abstract a greater number of F atoms from  $\text{SF}_6$  to form  $\text{SF}_n^+$  ( $n = 2, 5$ ).<sup>12</sup> Contrary to ionized  $\text{SF}_6$ , protonated sulfur hexafluoride is stable with respect to  $\text{HF}$  and  $\text{SF}_5^+$ .<sup>14</sup> Hence,  $\text{HSF}_6^+$  is formed in reactions of  $\text{SF}_6$  with several protonated molecules such as  $\text{CH}_5^+$ , which permitted the estimation of the proton affinity of  $\text{SF}_6$  via bracketing experiments.<sup>14</sup>

† In memoriam.

More diverse reactivity has been reported for gaseous  $\text{SF}_n^+$ ,<sup>15–23</sup> but studies also have been rather scattered. Neutral  $\text{SF}_6$  reacts with  $\text{SF}_n^+$  to form a number of “top-hat” coordinated, weakly bonded complexes of the  $\text{SF}_n(\text{SF}_6)_m^+$  ( $m = 0–5$ ;  $n = 1–3$ ) type.<sup>15</sup> In reactions of  $\text{SF}_5^+$  and  $\text{SF}_3^+$  with a series of amines,<sup>16</sup>  $\text{SF}_5^+$  was found to transfer  $\text{F}^+$ , whereas both  $\text{SF}_5^+$  and  $\text{SF}_3^+$  react by complex formation followed by HF elimination.  $\text{SF}_5^+$  forms a complex with  $\text{H}_2\text{S}$  that partially dissociates to  $\text{SF}_4\text{SH}^+$  by HF loss, and this reaction has been used to reevaluate the appearance energy  $\text{AE}(\text{SF}_5^+/\text{SF}_6)$  and the dissociation energy  $D(\text{SF}_5-\text{F})$ .<sup>17</sup> In a study of  $\text{SF}_6/\text{H}_2\text{O}$  mixtures at pressures of around 1 Torr and temperatures in the range of 350–500 K, the  $\text{SF}_5\cdot\text{H}_2\text{O}^+$  complex was formed and found to decompose slowly to  $\text{SF}_3\text{O}^+$ .<sup>18</sup> Reactions of  $\text{SF}_5^+$  with water and methanol under high-pressure mass spectrometric conditions were also observed to take place by complex formation followed by partial elimination of two HF molecules (or HF and  $\text{CH}_3\text{F}$ ) to yield  $\text{SF}_3\text{O}^+$ .<sup>19</sup> In the same study,<sup>19</sup>  $\text{SF}_5^+$  was found to form complexes with benzene, toluene, acetone, acetic acid, and nitriles, whereas the complexes with benzene and toluene eliminate HF at long reaction times. Ion bombardment of a polystyrene surface by gaseous  $\text{SF}_5^+$  causes fluorination, partial destruction of aromaticity, fluorination of the resulting non-aromatic organic material, and sputtering of the polystyrene.<sup>20</sup> An early study<sup>21</sup> showed that gas-phase reactions of  $\text{SF}_5^+$ ,  $\text{SF}_4^+$ , and  $\text{SF}_3^+$  with  $\text{O}_2$  and  $\text{NO}$  occur either by charge exchange or dissociation by F loss. Recently,<sup>22</sup> complexes and dimers of  $\text{SF}_3^+$  with pyridines have been formed in the collision cell of a pentaquadrupole mass spectrometer, and  $\text{SF}_3^+$  pyridine affinities were estimated via the application of the Cooks’ kinetic method.<sup>24</sup>  $\text{SF}_5^+$ ,  $\text{SF}_4^+$ ,  $\text{SF}_2^+$ , and  $\text{SF}^+$  were found, however, to be practically unreactive toward complex and dimer formation with pyridine.<sup>22</sup> Pentaquadrupole MS has also been applied in a recent study of the ability of  $\text{SF}_n^+$  to form stable complexes and dimers with benzene, acetonitrile, and pyridine.<sup>23</sup>

We report herein a systematic investigation on the gas-phase reactivity of the singly charged sulfur hexafluoride fragment ions  $\text{SF}_n^+$  ( $n = 0–5$ ) (more specifically  $^{32}\text{SF}_n^+$ ) and the doubly charged ions  $^{32}\text{SF}_n^{2+}$  ( $n = 2,4$ ) with  $\text{O}_2$  and the common oxygenated neutral gases  $\text{H}_2\text{O}$ ,  $\text{CO}$ ,  $\text{CO}_2$ , and  $\text{N}_2\text{O}$ . The study has been performed with “pure” (i.e., mass-selected) ions and under controlled low-energy collision conditions via multiple-stage pentaquadrupole (QqQqQ) mass spectrometry.<sup>25</sup> The main goal of the study was to test and compare the proclivity of each of the  $\text{SF}_n^+$  and  $\text{SF}_n^{2+}$  ions either to undergo oxidation via abstraction of an oxygen atom from the neutral gases or to form complexes with these potentially  $\pi$ -coordinating molecules. Theory, i.e., high level G2(MP2) ab initio thermochemistry, was used to help rationalize a number of interesting and contrasting chemical reactivities that were observed for the ions.

## Methods

The  $\text{MS}^2$  and  $\text{MS}^3$  experiments were performed using an Extrel (Pittsburgh, PA) pentaquadrupole (QqQqQ) mass spectrometer, which has been described in detail elsewhere.<sup>26</sup> Pentaquadrupole mass spectrometers, as represented schematically in Figure 1, are composed of a sequential arrangement of three mass-analyzing (Q1, Q3, Q5) and two radio-frequency-only “ion-focusing” reaction quadrupoles (q2, q4). This on-line arrangement allows the performance of a variety of *tandem-in-space* multidimensional  $\text{MS}^2$  and  $\text{MS}^3$  experiments, from which specific chemical information are derived.<sup>27,28</sup> QqQqQ’s have been shown to constitute suitable “laboratories” for gas-phase ion/molecule reaction studies,<sup>27</sup> a subject that has been recently reviewed.<sup>25</sup>

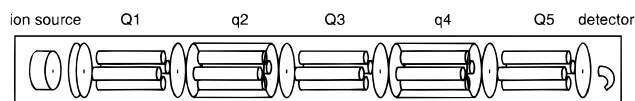


**Figure 1.** Schematic of the pentaquadrupole mass spectrometer, a versatile “laboratory” for gas-phase ion chemistry studies. Q1, Q3, and Q5 are mass-analyzing quadrupoles whereas the q2 and q4 quadrupoles function as ion-focusing reaction chambers. In a typical ion/molecule reaction experiment, ions are generated in the ion-source, purified (mass-selected) by Q1, and further reacted under controlled conditions (collision energy and pressure) with a neutral gas introduced in q2. Product ions of interest are then subsequently mass-selected by Q3 and structurally characterized by either collision-induced dissociation or structurally diagnostic ion/molecule reactions in q4, while Q5 is scanned to acquire the triple-stage mass spectra. For more details, see refs 25 and 26.

Ion/molecule reactions were performed in the pentaquadrupole by double-stage ( $\text{MS}^2$ ) experiments in which Q1 was used to select the ion of interest. Reactions were then performed in q2 with a chosen neutral reagent at near 0 eV collision energies and at neutral reagent pressures that were adjusted to maximize reaction yields. The  $\text{MS}^2$  product spectra were acquired by scanning Q5, while operating Q3 in the “full-transmission” rf-only mode.

For the triple-stage ( $\text{MS}^3$ ) experiments,<sup>28</sup> a product ion of interest formed in q2 was mass-selected by Q3 and further dissociated by 15 eV collisions with argon in q4, whereas Q5 was again scanned for spectrum acquisition. The total pressures inside each differentially pumped region were typically  $2 \times 10^{-6}$  (ion-source),  $8 \times 10^{-6}$  (q2), and  $8 \times 10^{-5}$  (q4) Torr, respectively. At these pressures, multiple collisions occur in the reaction quadrupoles, which increases reaction yields and helps to promote collisional “cooling” of the reactant ions.<sup>25</sup> It is important to note, however, that lower reaction yields but similar sets of ionic products were always observed at lower pressure, single collision conditions in q2. The collision energies were calculated as the voltage difference between the ion source and the collision quadrupoles.

Ab initio molecular orbital calculations were carried out by using Gaussian94<sup>29</sup> and the high-accuracy G2(MP2) model.<sup>30</sup> The G2(MP2) model adopts a composite procedure based effectively on QCISD-(T)/6-311G+(3df,2p)/MP2(full)/6-31G-(d) energies (evaluated by making certain additivity assumptions) together with ZPE and isogyric corrections and has been shown to produce results with high accuracy in various chemical systems.<sup>30</sup>

## Results and Discussion

**Collision Dissociation.**  $\text{SF}_n^+$ . Figure 2 shows the three-dimensional double-stage mass spectrum in which the most abundant ions formed upon dissociative 70 eV EI ionization of  $\text{SF}_6$  are displayed, each of them directly associated with their respective fragment ions. To acquire this 3D spectrum, two mass-analyzing quadrupoles (Q1 and Q3) were synchronously scanned<sup>26</sup> over mass-to-charge ( $m/z$ ) ranges of interest, while 15 eV collisional dissociation of the Q1 mass-selected ions were performed in the first collision quadrupole (q2). Synchronous scanning was performed by stepping Q1 one mass unit at a time while scanning Q3 along the entire mass range of interest at each setting of Q1. This 3D spectrum is particularly useful because it permits a quite adequate comparison of the relative dissociation proclivities of the  $\text{SF}_n^+$  ions; the *tandem-in-space* mode of operation of the QqQqQ permits that the same experimental collision conditions being applied to fragment, one at a time, each of the mass-selected ions. In Figure 2, the

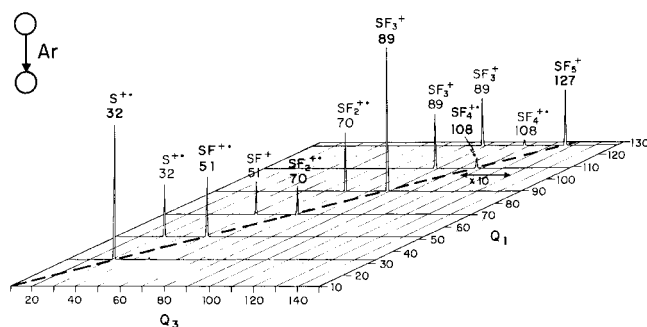


**Figure 2.** Three-dimensional double-stage mass spectrum that shows the entire domain of data for 15 eV collisional dissociation of the most abundant ions formed upon dissociative 70 eV electron ionization of  $\text{SF}_6$ . Note that the precursor  $\text{SF}_n^+$  ions are displayed along the dashed line ( $m/z_{Q1} = m/z_{Q3}$ ), and that each  $\text{SF}_n^+$  ion is directly associated with its respective fragment ions, which are seen across the  $Q3$  axis. Owing to the *tandem-in-space* mode of operation of the  $QqQqQ$ , the same experimental collision conditions were applied to fragment each of the mass-selected ions.

precursor ions that survive collisions with argon in  $q2$  are displayed along the dashed diagonal line, whereas the respective fragment ions are seen across the horizontal axis. Precursor ions are transmitted along the diagonal line since it defines the scanning conditions in which equal masses are simultaneously selected by both  $Q1$  and  $Q3$ .

Note in Figure 2 that the  $\text{SF}_n^+$  ( $n = 1-5$ ) ions, except  $\text{SF}_4^+$  and  $\text{SF}_5^+$ , dissociate to similar and medium extents by single F loss ( $\text{SF}_n^+ \rightarrow \text{SF}_{n-1}^+ + \text{F}$ ) under the collisions conditions employed.  $\text{SF}_4^+$ , however, dissociates much more promptly by F loss to afford  $\text{SF}_3^+$  of  $m/z$  89. The abundance in the 3D spectrum of the surviving precursor ion  $\text{SF}_4^+$  of  $m/z$  108 was so low that a 10-times expansion had to be used as to make its signal visible. Note also that dissociation of  $\text{SF}_5^+$ , owing to the ease of dissociation of its primary fragment  $\text{SF}_4^+$ , occurs predominantly by double F loss; hence,  $\text{SF}_3^+$  is seen as the most abundant fragment of  $\text{SF}_5^+$ .

**G2(MP2) Dissociation Thresholds.** The distinctive trends in dissociation behavior seen in Figure 2 for the  $\text{SF}_n^+$  ( $n = 1-5$ ) ions are easily rationalized when one compares their G2(MP2) ab initio dissociation thresholds for F loss (Table 1). These values are summarized in the potential energy surface diagram shown in Figure 3. Note that  $\text{SF}_6^{2+}$  is unstable with respect to dissociation to  $\text{SF}_5^{2+}$ ; hence, none of the intact molecular ion was sampled by  $Q1$ . Of the intrinsically stable  $\text{SF}_n^+$  ions ( $n = 1-5$ ),  $\text{SF}_4^+$  is unique as it displays a F loss dissociation threshold (13.0 kcal/mol) approximately eight to nine times lower than that of the other  $\text{SF}_n^+$  ions. Therefore,  $\text{SF}_4^+$  should dissociate much more promptly upon collision activation, as is indeed observed (Figure 2). The ease of dissociation of  $\text{SF}_4^+$  will likely prevent most of its associative reactions, as is exemplified by the ion/molecule reaction results discussed in the following section. Quite endothermic dissociation thresholds on the range of 80–100 kcal/mol are predicted, however, for  $\text{SF}_5^+$ ,  $\text{SF}_3^+$ ,  $\text{SF}_2^+$ , and  $\text{SF}^+$ ; hence, they are considerably more stable (than  $\text{SF}_4^+$ ) with respect to collision dissociation (Figure 2).

**$\text{SF}_n^{2+}$ .** Two minor doubly charged ions are formed upon 70 eV dissociative EI of  $\text{SF}_6$ , i.e.,  $\text{SF}_2^{2+}$  of  $m/z$  35 and  $\text{SF}_4^{2+}$  of  $m/z$  54. Owing to low abundance and a substantial noise filter used when acquiring the three-dimensional spectrum of Figure 2, the doubly charged ions were not sampled. Therefore, their collision dissociation spectra were collected separately (Figure 4). Likely owing to the high ionization energy of the corresponding singly charged ions, the doubly charged ions  $\text{SF}_2^{2+}$

**TABLE 1: Total Energy from G2(MP2) ab Initio Calculations**

species <sup>a</sup>	total energy (hartree)	species <sup>a</sup>	total energy (hartree)
$\text{SF}^+$	−497.028 50 <sup>a</sup>	$\text{CO}_2$	−188.356 62
$\text{SF}_2^+$	−596.808 78 <sup>a</sup>	$\text{SO}_2$	−548.007 09
$\text{SF}_3^+$	−696.590 58 <sup>a</sup>	$\text{SO}_2^{2+}$	−547.519 73
$\text{SF}_4^+$	−796.240 09 <sup>a</sup>	$\text{COS}$	−510.939 55
$\text{SF}_5^+$	−896.011 41 <sup>a</sup>	$\text{COS}^+$	−510.529 87
$\text{SF}_6^+$	unstable <sup>a,c</sup>	$\text{CO-F}^+$	−212.281 25
C	−37.783 90 <sup>b</sup>	$\text{F-CO}^+$	−212.518 25
O	−74.978 68 <sup>b</sup>	$\text{CO-SF}^+$	−610.196 30
$\text{O}^+$	−74.483 83 <sup>b</sup>	$\text{FS-CO}^+$	−610.274 95
S	−397.646 99 <sup>b</sup>	$\text{F-SO}^+$	−572.229 59
$\text{S}^+$	−397.276 39 <sup>b</sup>	$\text{F-SC}^+$	−534.974 09
F	−99.628 94 <sup>b</sup>	$\text{N}_2\text{O-F}^+$	−283.636 25
$\text{F}^+$	−98.991 08 <sup>b</sup>	$\text{N}_2\text{O-SF}^+$	−681.485 25
CO	−113.175 40 <sup>b</sup>	$\text{FS-O}_2^+$	−647.202 31
$\text{CO}^+$	−112.660 32 <sup>b</sup>	$\text{O}_2\text{-F}^+$	−249.349 07
$\text{O}_2$	−150.142 08 <sup>b</sup>	$\text{SF}_2\text{O}^+$	−671.899 34
$\text{N}_2$	−109.389 48 <sup>b</sup>	$\text{SF}_3\text{O}^+$	−771.704 23
SO	−472.819 30 <sup>b</sup>	$\text{CO}_2\text{S}^+$	−585.632 25
$\text{SO}^+$	−472.444 36	$\text{N}_2\text{O-SF}_2^{2+}$	unstable <sup>d</sup>
$\text{N}_2\text{O}$	−184.432 47	$\text{N}_2\text{O-SF}_3^+$	unstable <sup>d</sup>

<sup>a</sup> Data taken from ref 9. <sup>b</sup> Data taken from ref 30. <sup>c</sup> Equilibrium structure for  $\text{SF}_6^{2+}$  was not found; see ref 9. <sup>d</sup> With respect to  $\text{N}_2\text{O}$  and the  $\text{SF}_n^+$  ion.

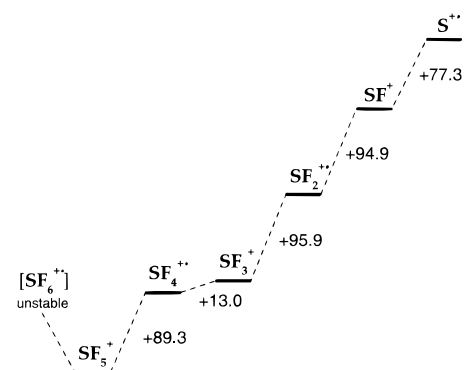


**Figure 3.** G2(MP2) energy thresholds (in kcal/mol) of  $\text{SF}_n^+$  ions. Note that  $\text{SF}_6^{2+}$  is an intrinsically unstable species that dissociates spontaneously by F loss to  $\text{SF}_5^{2+}$ . Note also the relatively low dissociation threshold of  $\text{SF}_4^+$ .

and  $\text{SF}_4^{2+}$  promptly undergo charge exchange with argon (or with other residual gases present in  $q2$ ) to form the corresponding singly charged ions  $\text{SF}_2^+$  ( $m/z$  70) and  $\text{SF}_4^+$  ( $m/z$  108).  $\text{SF}_2^+$  dissociates in turn partially to  $\text{SF}^+$  of  $m/z$  51, whereas  $\text{SF}_4^+$ , as expected from its very low dissociation threshold (Figure 3), dissociates completely to  $\text{SF}_3^+$  ( $m/z$  89) and  $\text{SF}_2^+$  ( $m/z$  70).

**Ion/Molecule Chemistry.** *Reactions with  $\text{O}_2$  and Other Oxygenated Gases.* Table 2 summarizes the results for reactions of mass-selected  $^{32}\text{SF}_n^+$  and  $^{32}\text{SF}_n^{2+}$  with  $\text{H}_2\text{O}$ ,  $\text{CO}$ ,  $\text{CO}_2$ ,  $\text{O}_2$ , and  $\text{N}_2\text{O}$ , i.e., possible oxidizing or  $\pi$ -coordinating molecules. The double-stage product spectra for some of the most representative cases are shown as figures as indicated in the following text. Most collision processes did not lead to reactions, and dissociation of the ions by F loss took place predominantly even under the very low energy collisions employed (Table 2). F loss was always the main process for the higher homologues  $\text{SF}_5^+$ ,  $\text{SF}_4^+$ ,  $\text{SF}_3^+$  and  $\text{SF}_2^+$ , whereas charge exchange followed by the respective dissociation of the corresponding singly charged ion (see Figure 4) was the only reaction channel observed for the doubly charged ions  $\text{SF}_n^{2+}$  (Table 2).



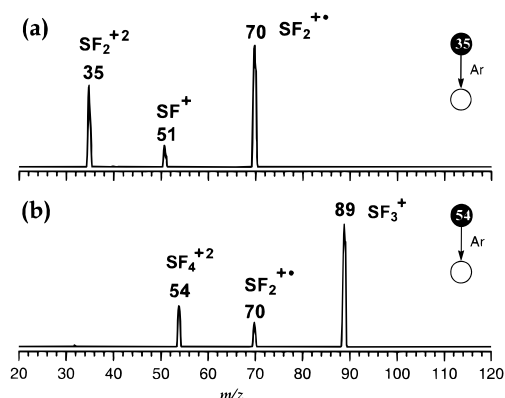


**Figure 4.** Double-stage ( $MS^2$ ) 15 eV collisional-induced dissociation product spectra of (a)  $SF_4^{2+}$  and (b)  $SF_2^{2+}$ . In the terminology used to describe the type of  $MS^n$  experiment and scan mode employed, a filled circle represents a fixed (or selected) mass and; an open circle, a variable (or scanned) mass, whereas the neutral reagent or collision gas that causes the mass transitions is shown between the circles. For more details on this terminology, see ref 28.

**TABLE 2: Major Product Ion or Ionic Fragment Formed upon Low-Energy (Near Zero) Multiple Collisions of  $SF_n^+$  and  $SF_n^{2+}$  with  $O_2$  and Other Oxygen-Containing Neutral Molecules**

	$S^{+*}$	$SF^+$	$SF_2^{+*}$	$SF_3^+$	$SF_4^{+*}$	$SF_5^+$	$SF_2^{2+}$	$SF_4^{2+}$
$H_2O$	NR <sup>a</sup>	$S^{+*}$	$SF^+$	$SF_2^{+*}$	$SF_3^+$	$SF_3^+$	$SF_2^{+*}$	$SF_3^{+d}$
$CO$	$SO^{+*b}$	$SCO^{+*}$	$SF^+$	$SF_2^{+*}$	$SF_3^+$	$SF_3^+$	$SF_2^{+*}$	$SF_3^{+d}$
$CO_2$	$SO^{+*}$	$S^{+*}$	$SF^+$	$SF_2^{+*}$	$SF_3^+$	$SF_3^+$	$SF_2^{+*}$	$SF_3^{+d}$
$O_2$	$SO^{+*}$	$F-SO^+$	$SF^+$	$SF_2^{+*}$	$SF_3^+$	$SF_3^+$	$SF_2^{+*}$	$SF_3^{+d}$
$N_2O$	$N_2O^{+*c}$	$F-SO^+$	$SF^+$	$SF_2^{+*}$	$SF_3^+$	$SF_3^+$	$SF_2^{+*}$	$SF_3^{+d}$

<sup>a</sup> No ionic products were detected. <sup>b</sup>  $SO^{+*}$  is formed as a very minor product. <sup>c</sup>  $SO^{+*}$  is also formed but as a very minor product. <sup>d</sup> The corresponding ionized neutral is also formed.

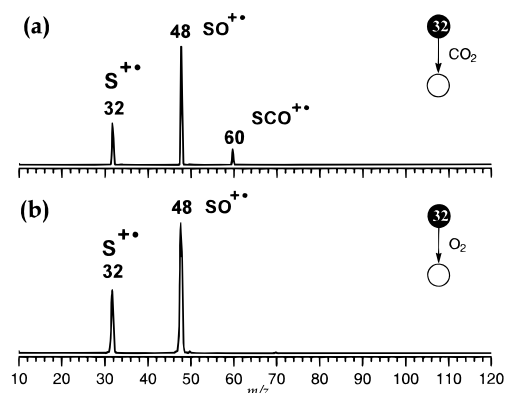


**Figure 5.** Double-stage ( $MS^2$ ) product spectra for reaction of  $^{32}S^{+*}$  of  $m/z$  32 with (a)  $CO_2$  and (b)  $O_2$ . Note the abundant product of O-abstraction ( $SO^{+*}$ ) of  $m/z$  48, which is formed in both reactions, and the minor CO-abstraction product ( $SCO^{+*}$ ) of  $m/z$  60 in (a).

The lower homologues  $SF^+$  and  $S^{+*}$ , however, are found to display a much richer reactivity with several of the neutral gases employed (Figure 5). Novel O-abstraction reactions occur to considerable extents upon collisions of  $S^{+*}$  with  $CO_2$  (Figure 5a) and  $O_2$  (Figure 5b), and of  $SF^+$  with  $O_2$  (Figure 6b) and  $N_2O$  (Figure 6c). In addition to O-abstraction, an interesting but considerably less favorable<sup>31</sup> CO-abstraction reaction that yields ionized carbon oxysulfide ( $COS^{+*}$ ) of  $m/z$  60 also occurs to a minor extent upon collisions of  $S^{+*}$  with  $CO_2$  (Figure 5a). The reactions just discussed and their corresponding G2(MP2) ab initio thermochemistry are summarized in Table 3, entries 1–6.

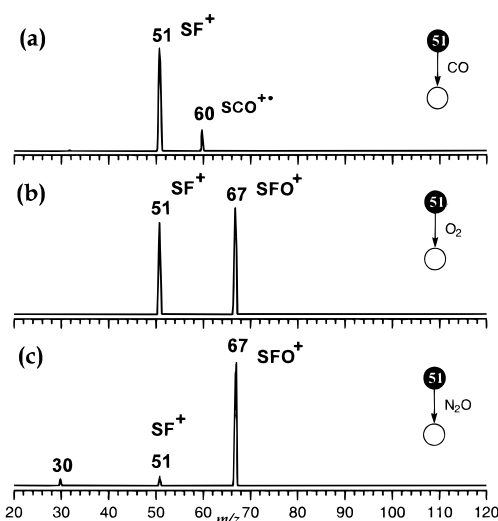


**Figure 6.** Double-stage ( $MS^2$ ) product spectra for reaction of  $^{32}SF^+$  of  $m/z$  51 with (a)  $CO$ , (b)  $O_2$ , and (c)  $N_2O$ . Note the relatively minor product of  $S^{+*}$  transfer ( $SCO^{+*}$ ) of  $m/z$  60 in (a) and the abundant O-abstraction product ( $F-SO^+$ ) of  $m/z$  60 in both (b) and (c).

**TABLE 3: G2(MP2) Enthalpy Changes at 0 K for Most Relevant Reaction and Dissociation Processes**

entry	process	$\Delta H_{0K}$ (kcal/mol)
1	$S^{+*} + CO_2 \rightarrow SO^{+*} + CO$	+8.3
2	$S^{+*} + CO_2 \rightarrow SCO^{+*} + O$	+77.6
3	$S^{+*} + O_2 \rightarrow SO^{+*} + O$	-16.3
4	$SF^+ + CO \rightarrow SCO^{+*} + F$	+28.3
5	$SF^+ + O_2 \rightarrow FSO^+ + O$	-23.9
6	$SF^+ + N_2O \rightarrow FSO^+ + N_2$	-99.2
7	$F-SO^+ \rightarrow F + SO^{+*}$	+98.1
8	$F-SO^+ \rightarrow F + SO$	+263.1
9	$F-SO^+ \rightarrow SF^+ + O$	+139.6
10	$COS^{+*} \rightarrow S^{+*} + CO$	+49.0
11	$COS^{+*} \rightarrow S + CO^{+*}$	+139.7
12	$COS^{+*} \rightarrow C + SO^{+*}$	+189.3
13	$SO^{+*} \rightarrow S^{+*} + O$	+118.8
14	$SO^{+*} \rightarrow S + O^{+*}$	+196.7
15	$SF_2^{+*} + CO_2 \rightarrow SF_2O^{+*} + CO$	+56.9
16	$SF_2^{+*} + O_2 \rightarrow SF_2O^{+*} + O$	+45.7
17	$SF_2^{+*} + N_2O \rightarrow SF_2O^{+*} + N_2$	-29.8
18	$SF_3^+ + CO_2 \rightarrow SF_3O^+ + CO$	+42.4
19	$SF_3^+ + O_2 \rightarrow SF_3O^+ + O$	+31.2
20	$SF_3^+ + N_2O \rightarrow SF_3O^+ + N_2$	-44.3

Another novel reaction for  $SF^+$ , i.e., sulfur cation ( $S^{+*}$ ) transfer, occurs to a moderate extent upon collisions with  $CO$  (Figure 6a). Note, therefore, the diverse reactivity of  $SF^+$  and  $S^{+*}$ ; i.e.,  $SF^+$  is unreactive toward  $CO_2$  and  $H_2O$ , reacts moderately by  $S^{+*}$  transfer with  $CO$ , and extensively by O-abstraction with  $O_2$  and  $N_2O$ .  $S^{+*}$ , on the other hand, reacts extensively with  $CO_2$  and  $O_2$  via O-abstraction and undergoes mainly charge exchange with  $N_2O$  (Table 2), whereas it is practically unreactive with  $H_2O$  and  $CO$ . Most trends in chemical reactivity of both  $SF^+$  and  $S^{+*}$  are easily rationalized on the basis of G2(MP2) ab initio thermochemistry of the respective reactions and competitive processes; see the ab initio section that follows.

**Triple-Stage ( $MS^3$ ) Spectra.** The multiple ion-selection/reaction capabilities of the pentaquadrupole mass spectrometer<sup>26</sup> permit “on-line” and straightforward access to structural information of reaction products via the recording of their sequential product spectra.<sup>28</sup> Acquisition of such spectra was accomplished by Q3 mass selection of a product ion formed in q2, which was in turn subjected to 15 eV dissociative collisions with argon in q4, whereas Q5 was scanned across appropriate  $m/z$  ranges.

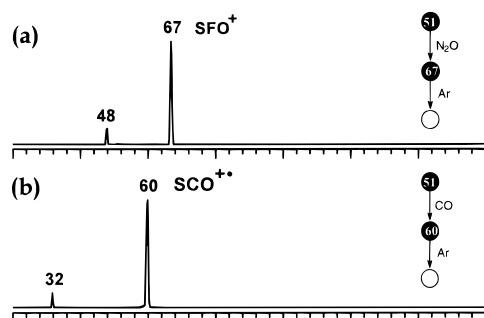


**Figure 7.** Triple-stage ( $\text{MS}^3$ ) sequential product spectra for (a) the O-abstraction product ( $\text{F-SO}^+$  of  $m/z$  67) formed in reactions of  $\text{SF}^+$  with  $\text{N}_2\text{O}$  and (b) the  $\text{S}^+$  transfer product ( $\text{SCO}^+$  of  $m/z$  60) formed in reactions of  $\text{SF}^+$  with  $\text{CO}$ . Similar triple-stage spectrum (not shown) was obtained for the O-abstraction product  $\text{F-SO}^+$  formed in reactions of  $\text{SF}^+$  with  $\text{O}_2$ .

The identity of the most relevant products ions could be established by such spectra. The sulfinyl cation<sup>32</sup>  $\text{F-SO}^+$  dissociates, as expected from its dissociation thresholds (see the *ab initio* section that follows), by F loss to form  $\text{SO}^+$  of  $m/z$  48 (Figure 7a). As expected from its dissociation thresholds (see below) and 70 eV EI dissociative behavior,<sup>33</sup>  $\text{SCO}^+$  (Figure 7b) dissociates mainly by CO loss to form  $\text{S}^+$  of  $m/z$  32. Ionized sulfur monoxide ( $\text{SO}^+$ ) dissociates barely by O loss to form  $\text{S}^+$  of  $m/z$  32 (spectrum not shown).

**G2(MP2) *ab Initio* Calculations.** Reliable thermochemical data are among the most useful information for chemical species and are used to predict chemical reactivity. The G2(MP2) *ab initio* model<sup>30</sup> has been shown to yield accurate thermochemical data for a variety of chemical species, with very narrow deviations from experiment, and its successful application to predict thermochemical properties of  $\text{SF}_n^+$  ions has been recently reported.<sup>9</sup> Therefore, G2(MP2) calculations have been performed for the most relevant cases to evaluate the thermochemistry of several possible competitive reactions and to better rationalize the contrasting reactivity displayed by the  $\text{SF}_n^+$  ions, as well as to corroborate most favorable reaction pathways. The G2(MP2) energies are collected in Table 1, whereas the enthalpy changes at 0K for the observed reactions are presented in Table 3, entries 1–6.

**Dissociation Thresholds.** Entries 7–14 of Table 3 also summarize the G2(MP2) *ab initio* thresholds for most likely dissociations of  $\text{F-SO}^+$ ,  $\text{SCO}^+$ , and  $\text{SO}^+$ . Note that the same dissociation processes observed in the triple-stage mass spectra of these ions are the ones predicted by the calculations to display the lower energy thresholds, i.e., F loss for  $\text{F-SO}^+$  (entry 7), CO loss for  $\text{SCO}^+$ , (entry 10) and O loss for  $\text{SO}^+$  (entry 13).

**$\text{SF}^+$  Reactions: O-Abstraction versus  $\text{S}^+$  Transfer.** Figure 8 presents G2(MP2) potential energy surface diagrams for the reaction of  $\text{SF}^+$  with CO,  $\text{O}_2$ , and  $\text{N}_2\text{O}$ . Most feasible reaction pathways have been considered. In reactions of  $\text{SF}^+$  with CO, primary reactions could occur via  $\text{F}^+$  transfer to CO with the formation of either  $\text{CO-F}^+$  or  $\text{F-CO}^+$ , or by complex formation ( $\text{CO}^+-\text{SF}$  or  $\text{FS-CO}^+$ ). The  $\text{CO-SF}^+$  complex could dissociate in turn by C loss to form  $\text{F-SO}^+$  as the product of a net O-abstraction reaction. The other possible adduct,  $\text{FS-CO}^+$ , could dissociate either by SCO loss to yield  $\text{F}^+$  ( $\text{S}^+$  transfer), by O loss to form  $\text{FSC}^+$  (C-abstraction), or by F loss to form ionized carbon oxysulfide  $\text{COS}^+$  ( $\text{S}^+$  transfer). As seen in Figure 8a, the  $\text{FS-CO}^+$  complex is predicted to be formed by the far most favorable, i.e., the only exothermic (−44.6 kcal/mol) primary reaction. The lowest dissociation threshold (+72.9 kcal/mol) for further dissociation of  $\text{FS-CO}^+$

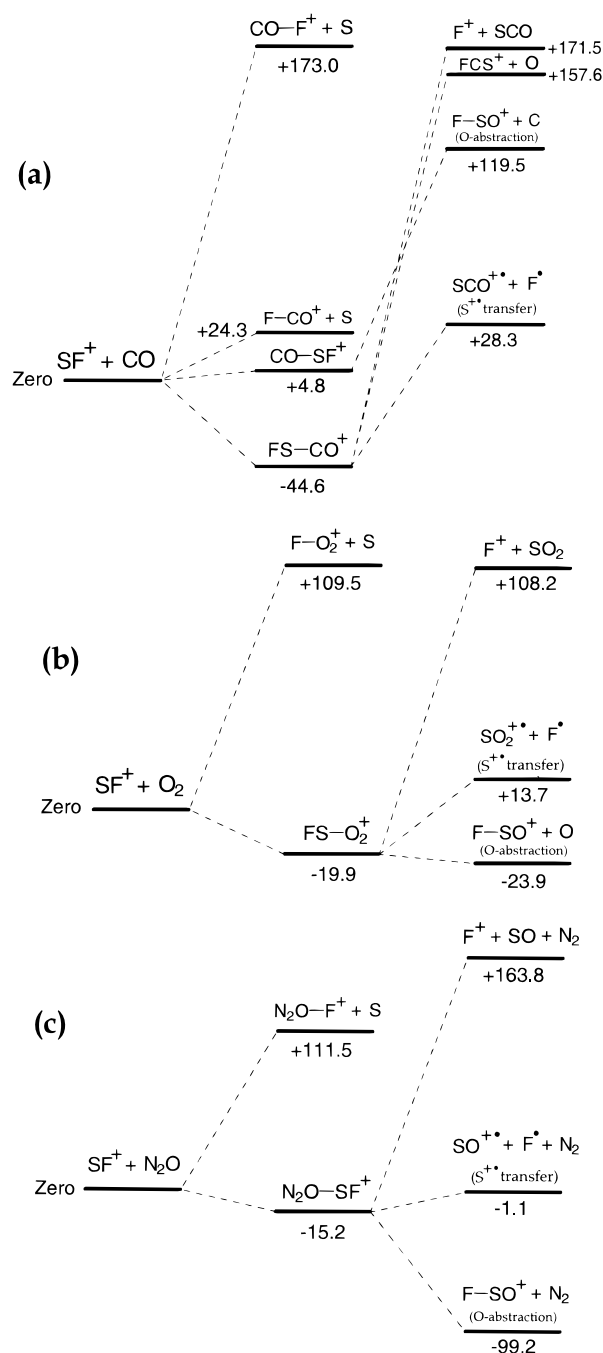


**Figure 8.** G2(MP2) *ab initio* partial potential energy reaction surface diagrams for reaction of  $\text{SF}^+$  with (a) CO, (b)  $\text{O}_2$ , and (c)  $\text{N}_2\text{O}$ . Energies are given in kcal/mol. Note that  $\text{S}^+$  transfer is suggested by the calculations as a not so effective (endothermic) but most likely reaction between the ion and CO, whereas the most exothermic, and therefore more thermodynamically favorable, reaction between  $\text{SF}^+$  with both  $\text{O}_2$  and  $\text{N}_2\text{O}$  is O-abstraction. The chemical reactivity of the ion reflects clearly these theoretical predictions; see Figure 6.

is that of F loss, which yields  $\text{SCO}^+$  (the observed product, Figure 6a). F loss is therefore expected to be the dominant process for the  $\text{FS-CO}^+$  adduct. Formation of  $\text{COS}^+$  is, however, predicted to be not so favorable since the reaction is overall +23.3 kcal/mol endothermic.

The potential energy surface diagram for reactions of  $\text{SF}^+$  with  $\text{O}_2$  (Figure 8b) suggests a different reactivity.  $\text{S}^+$  transfer reaction that yields  $\text{SO}_2^+$  is endothermic by 13.7 kcal/mol, whereas O-abstraction that yields  $\text{F-SO}^+$  is the most exothermic (−23.9 kcal/mol), thus thermodynamically favorable reaction.

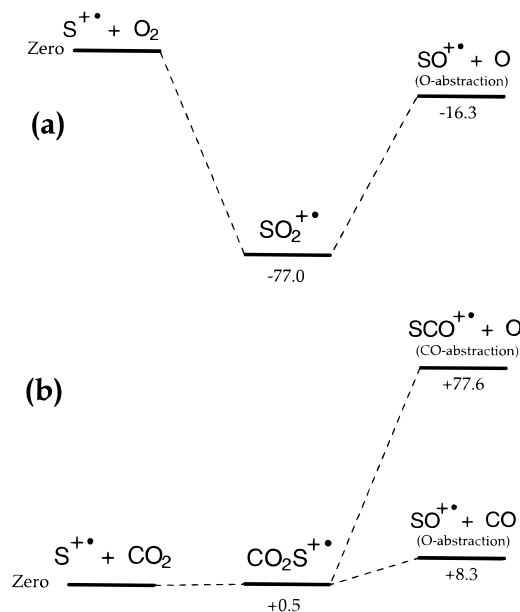


**Figure 9.** G2(MP2) ab initio partial potential energy reaction surface diagrams for reaction of  $S^{+\bullet}$  with (a)  $O_2$  and (b)  $CO_2$ . Energies are given in kcal/mol. Note that O-abstraction is suggested by the calculations to be considerably exothermic with  $O_2$  and slightly endothermic with  $CO_2$ .

Again, theory and experiment matches perfectly as the  $F-SO^+$  ion is formed as the exclusive ionic product in  $SF^+/O_2$  reactions (Figure 6b). Similar results, i.e., clear preference for O-abstraction ( $-99.2$  kcal/mol exothermic), which are again perfectly consistent with the experimental results (Figure 6c), are predicted for the  $SF^+/N_2O$  reaction (Figure 8c). Even the  $SF^+$  reactivity order,  $CO < O_2 < N_2O$  (estimated from the product ion/reactant ion abundance ratios,<sup>31</sup> see Figure 6), is consistent with the corresponding G2(MP2) thermochemistry; i.e., the moderate  $S^{+\bullet}$  transfer of  $SF^+$  to CO is predicted to be not as effective owing to its endothermicity by  $+28.3$  kcal/mol, whereas the extensive O-abstraction reactions of  $SF^+$  with  $O_2$  ( $-23.9$  kcal/mol) and  $N_2O$  ( $-99.2$  kcal/mol) are predicted to occur much more promptly and to be considerably and increasingly exothermic.

**O-Abstraction by  $S^{+\bullet}$ .** G2(MP2) calculations predict association of  $S^{+\bullet}$  with  $O_2$  that yields  $SO_2^{+\bullet}$  to be exothermic by as much as  $-77.0$  kcal/mol (Figure 9a). Enough energy is therefore available for the nascent  $SO_2^{+\bullet}$  to surpass the  $+60.7$  kcal/mol energy threshold predicted for its further dissociation by O loss. Thus, O-abstraction that affords  $SO^+$  is overall exothermic by  $-16.3$  kcal/mol (Figure 9a). Association of  $S^{+\bullet}$  with  $CO_2$  is predicted to be nearly isothermic (Figure 9b), whereas further dissociation of the  $CO_2S^{+\bullet}$  complex by CO loss to afford the main product  $SO^+$  (Figure 5a) displays a quite low dissociation threshold of  $+7.8$  kcal/mol. Net O-abstraction of  $S^{+\bullet}$  from  $CO_2$  is therefore just slightly endothermic by  $+8.3$  kcal/mol. On the other hand, the minor CO-abstraction that takes place in  $S^{+\bullet}/CO_2$  reactions ( $SCO^+$  in Figure 5a) is predicted to be a much more energy demanding process ( $+77.6$  kcal/mol, Figure 9b).

**$SF_2^{+\bullet}$  and  $SF_3^{+\bullet}$ .** Entries 15–20 of Table 3 summarize the G2(MP2) thermochemistry predicted for O-abstractions of  $SF_2^{+\bullet}$  and  $SF_3^{+\bullet}$  from  $CO_2$ ,  $O_2$ , and  $N_2O$ . Note that whereas the lack of O-abstraction reactivity for these ions (Table 2) with both  $CO_2$  and  $O_2$  can be rationalized in terms of considerably endothermic reactions (entries 15, 16, 18, and 19), O-abstractions of both  $SF_2^{+\bullet}$  (entry 17) and  $SF_3^{+\bullet}$  (entry 20) from  $N_2O$  with

the consequent release of the stable  $N_2$  molecule are, however, predicted to be overall quite exothermic. Because these reactions did not take place under the collision conditions employed (Table 2), it is suggested that they must be hampered by unfavorable, much too endothermic primary association reactions. The G2(MP2) results support this assumption as the corresponding  $SF_2^{+\bullet}$  and  $SF_3^{+\bullet}$  complexes with  $N_2O$  are found to be unstable with respect to the starting reactants (Table 1).

## Conclusion

A combined theoretical and experimental systematic study on the gas-phase chemistry of the  $SF_6$  fragment ions  $SF_n^+$  and  $SF_n^{2+}$  with a series of oxygenated neutral gases has been carried out. Whereas the higher homologues  $SF_5^+$ ,  $SF_4^{+\bullet}$ ,  $SF_3^+$ , and  $SF_2^{+\bullet}$  and the doubly charged ions  $SF_4^{2+}$  and  $SF_2^{2+}$  undergo mainly charge exchange or dissociation by F loss, or both, novel reactions have been experimentally observed and theoretically suggested for the lower homologues  $SF^+$  and  $S^{+\bullet}$ .  $SF^+$  abstracts efficiently an oxygen atom from  $O_2$  and  $N_2O$ , and the corresponding oxyion  $F-SO^+$  is formed. O-abstraction also occurs extensively in reactions of  $S^{+\bullet}$  with  $CO_2$  and  $O_2$ , and ionized sulfur monoxide ( $SO^+$ ) is formed. A novel but less favorable sulfur cation ( $S^{+\bullet}$ ) transfer that affords ionized carbon oxysulfide ( $COS^+$ ) also occurs in reactions of  $SF^+$  with CO. When making comparisons with the other  $SF_n^+$  ions,  $SF_4^{+\bullet}$  was found (both by experiment and theory) to display a much lower F loss dissociation threshold. It is therefore likely that the ease of dissociation of  $SF_4^{+\bullet}$  will prevent most of its associative reactions.

$SF_6$  and its  $SF_n^+$  fragment ions are of practical and fundamental interest, and the chemical reactivity with the oxygenated gases described herein may help to rationalize and control the many processes in which  $SF_n^+$  participates. For instance, in applications of  $SF_6$  in which  $SF_n^+$  ions are formed, the present results point to the two lowest congeners  $SF^+$  and  $S^{+\bullet}$  as the most reactive species. Reactions of  $SF^+$  with residual  $O_2$ , and of  $S^{+\bullet}$  with residual  $O_2$  or  $CO_2$ , are therefore possible routes for  $SF_6$  degradation.

**Acknowledgment.** This paper is specially dedicated to Prof. José Carlos Nogueira (in memoriam) for his incisive contribution to physical chemistry in Brazil and for his initial plannings of the present work. Support from the Research Support Foundation of the State of São Paulo (FAPESP) and the Brazilian National Research Council (CNPq) is greatly acknowledged.

## References and Notes

- (1) Sauers, I.; Ellis, H. W.; Christophorou, L. G. *IEEE Trans. Electr. Insul.* **1986**, EI-21, 111.
- (2) Cob, J. W. *Plasma Chem. Plasma Process.* **1982**, 2, 1.
- (3) Stone, J. A.; Wytenberg, W. J. *Int. J. Mass Spectrom. Ion Proc.* **1989**, 94, 269.
- (4) (a) Babcock, L. M.; Streit, G. E. *J. Chem. Phys.* **1981**, 75, 3868. (b) Lyman, J. L.; Jensen, R. J. *J. Phys. Chem.* **1973**, 77, 883. (c) Chen, C. L.; Chantry, P. J. *J. Chem. Phys.* **1979**, 71, 2897.
- (5) (a) Grant, E. R.; Coggiola, M. J.; Lee, Y. T.; Schulz, P. A.; Subdo, Aa. S.; Shen, Y. R. *Chem. Phys. Lett.* **1977**, 52, 595. (b) Lyman, L. J. *Chem. Phys.* **1977**, 67, 1868.
- (6) McAlpine, R. D.; Evans, D. K. *Adv. Chem. Phys.* **1985**, 60, 31.
- (7) Mitchell, K. A. *Chem. Rev.* **1969**, 69, 157.
- (8) Pauling, L. *The Nature of The Chemical Bond*, 3rd ed.; Cornell University Press: Ithaca, NY, 1960.
- (9) Cheung, Y.-S.; Chen, Y.-J.; Ng, C. Y.; Chiu, S.-W.; Li, W.-K. *J. Am. Chem. Soc.* **1995**, 117, 9725. (b) Irikura, K. K.; *J. Chem. Phys.* **1995**, 102, 5357 and references therein.

- (10) (a) Wang, H.-X.; Moore, J. H.; Olthoff, J. K.; Van Brunt, R. J. *Plasma Chem. Plasma Process.* **1993**, 13, 1. (b) van Brunt, R. J.; Herron, J. T. *IEEE Trans. Electr. Insul.* **1990**, 25, 76.
- (11) Tamura, A.; Inoue, K.; Onuma, T.; Sato, M. *Appl. Phys. Lett.* **1987**, 51, 1503.
- (12) Jiao, C. Q.; Freiser, B. S. *J. Am. Chem. Soc.* **1993**, 115, 6268.
- (13) (a) Babcock, L. M.; Streit, G. E. *J. Chem. Phys.* **1981**, 74, 5700. (b) Tichy, M.; Javahery, G.; Twiddy, N. D. *Int. J. Mass Spectrom. Ion Processes* **1987**, 79, 231. (c) Shul, R. J.; Upshulte, B. L.; Passarella, R.; Keesee, R. G.; Castleman, A. W., Jr. *J. Phys. Chem.* **1987**, 91, 2556. (d) Fehsenfeld, F. C. *J. Chem. Phys.* **1971**, 54, 438. (e) Richter, R.; Tosi, P.; Lindinger, W. *J. Chem. Phys.* **1987**, 87, 4615.
- (14) (a) Latimer, D. R.; Smith, M. A. *J. Chem. Phys.* **1994**, 101, 3410. (b) Mackay, G. I.; H. I. Schiff, Bohme, D. K. *Int. J. Mass Spectrom. Ion Processes* **1992**, 117, 387.
- (15) Hiraoka, K.; Shimizu, A.; Minamitsu, A.; Nasu, M.; Fujimaki, S.; Yamabe, S. *J. Am. Soc. Mass Spectrom.* **1995**, 6, 1137.
- (16) Dillard, J. G.; Troester, J. H. *J. Phys. Chem.* **1975**, 79, 2455.
- (17) (a) Zangerle, R.; Hansel, A.; Richter, R.; Lindinger, W. *Int. J. Mass Spectrom. Ion Processes* **1993**, 129, 117. (b) Richter, R.; Tosi, P.; Lindinger, W. *J. Chem. Phys.* **1993**, 87, 4615.
- (18) Karachevtev, A. Z.; Maratkin, A. Z.; Savkin, V. V.; Tal'rose, V. L. *Sov. J. Chem. Phys.* **1985**, 3, 695.
- (19) Stone, J. A.; Wytenberg, W. J. *Int. J. Mass Spectrom. Ion Processes* **1989**, 280, 269.
- (20) Komienko, O.; Ada, E. T.; Hanley, L. *Anal. Chem.* **1997**, 69, 1536.
- (21) Fehsenfeld, F. C. *J. Chem. Phys.* **1971**, 54, 438.
- (22) Wong, P. S. H.; Ma, S.; Yang, S. S.; Cooks, R. G.; Gozzo, F. C.; Eberlin, M. N. *J. Am. Soc. Mass Spectrom.* **1996**, 8, 68.
- (23) Sparrapan, R.; Mendes, M. A.; Eberlin, M. N. *J. Phys. Chem. A*, submitted for publication.
- (24) (a) Cooks, R. G.; Patrick, J. S.; Kotiaho, T.; McLuckey, S. A. *Mass Spectrom. Rev.* **1994**, 13, 287. (b) Eberlin, M. N.; Kotiaho, T.; Shay, B. J.; Yang, S. S.; Cooks, R. G. *J. Am. Chem. Soc.* **1994**, 116, 2457. (c) Wong, P. S. H.; Ma, S.; Yang, S. S.; Gozzo, F. C.; Eberlin, M. N. *J. Am. Soc. Mass Spectrom.* **1997**, 8, 68.
- (25) Eberlin, M. N. *Mass Spectrom. Rev.* **1997**, 16, 113.
- (26) Juliano, V. F.; Gozzo, F. C.; Eberlin, M. N.; Kascheres, C.; Lago, C. L. *Anal. Chem.* **1996**, 68, 1328.
- (27) (a) Sorrilha, A. E. P. M.; Gozzo, F. C.; Pimpim, R. S.; Eberlin, M. N. *J. Am. Soc. Mass Spectrom.* **1996**, 7, 1126. (b) Eberlin, M. N.; Sorrilha, A. E. P. M.; Gozzo, F. C.; Sparrapan, R. *J. Am. Chem. Soc.*, **1997**, 119, 3550. (c) Moraes, L. A. B.; Pimpim, R. S.; Eberlin, M. N. *J. Org. Chem.* **1996**, 61, 8726. (d) Moraes, L. A. B.; Gozzo, F. C.; Eberlin, M. N.; Vainiotalo, P. *J. Org. Chem.* **1997**, 62, 5096. (e) Carvalho, M.; Sparrapan, R.; Mendes, M. A.; Kascheres, C.; Eberlin, M. N. *Chem. Eur. J.* **1998**, 4, 1159.
- (28) Schwartz, J. C.; Wade, A. P.; Enke, C. G.; Cooks, R. G. *Anal. Chem.* **1990**, 62, 1809.
- (29) Frisch, M. J.; Trucks, G. W.; Schlegel, H. B.; Gill, P. M. W.; Johnson, B. G.; Robb, M. A.; Cheeseman, J. R.; Keith, T.; Petersson, G. A.; Montgomery, J. A.; Raghavachari, K.; Al-Laham, M. A.; Zakrzewski, V. G.; Ortiz, J. V.; Foresman, J. B.; Peng, C. Y.; Ayala, P. Y.; Chen, W.; Wong, M. W.; Andres, J. L.; Replogle, E. S.; Gomperts, R.; Martin, R. L.; Fox, D. J.; Binkley, J. S.; Defrees, D. J.; Baker, J.; Stewart, J. P.; Head-Gordon, M.; Gonzalez, C.; Pople, J. A. *GAUSSIAN94*, Revision B.3; Gaussian, Inc.: Pittsburgh, PA, 1995.
- (30) Curtis, L. A.; Raghavachari, K.; Pople, J. A. *Gaussian94*, Revision B.3; *J. Chem. Phys.* **1993**, 98, 1293.
- (31) Considering that similar collision conditions are applied for all reactions, the ratio of the sum of the abundance of the ionic products to that of the surviving reactant ion is used as an (rough) estimate of relative reactivities.
- (32) Gozzo, F. C.; Eberlin, M. N. *J. Mass Spectrom.* **1995**, 30, 1553.
- (33) McLafferty, F. W.; Stauffer, D. D. *The Wiley/NBS Registry of Mass Spectral Data*; Wiley: New York, 1989; Vol. 1.